Scientia Iranica, Vol. 12, No. 4, pp 442–454

SCIENTIA IRANICA

Research Note

Limit Load Analyses of Plates with a Hole Under in-Plane Loads

G.H. Rahimi* **and R.A. Alashti**[1]

In this paper, the results of limit analyses are presented in dimensionless form for a wide range of geometric parameters, which are practically of interest. Analytical estimation of upper bound and lower bound limit loads of a plate with an elliptical hole under uniaxial loading and with a circular hole under biaxial loading in-plane stress condition are calculated; the analytical results are then compared with finite element calculations and the correlation between them is discussed. The finite element calculations consist of elastic-plastic estimation of limit load and lower and upper bound limit load prediction, using the elastic compensation method. The analytical upper and lower bound estimations and elastic-plastic results are found to be in good agreement with elastic compensation lower bound values, while the elastic compensation upper bound results are found to be overestimated.

INTRODUCTION

The determination of stress concentration, due to holes, notches and changes of section under various loading conditions is a question of considerable practical importance. The stress concentration problem of a circular hole in a plate subjected to uniformly distributed edge stress was first studied by Kirsch [1]. An extensive discussion on stress concentration problems is given by Savin [2] and stress concentration factors for a wide range of geometries are tabulated by Peterson [3]. Chong and Pinter [4] employed the finite element method to investigate the effect of a hole diameter to the width of strip on the stress concentration factor for a plate subjected to uniformly distributed edge stress. Many authors have also studied the limit loads of plates with circular holes under various loading conditions. In the early fifties, P.G. Hodge Jr and R.K. Froyd [5] examined the reinforcement to full strength of a thin slab with a slit. P.G. Hodge Jr [6] had introduced a final report on the yield loads of slabs with reinforced cutouts and discussed various subjects concerning limit analysis in [7,8]. F.A. Gaydon and A.W. McCrum [9,10] published their work on theoretical investigation of the yield point loading of a square plate with a central circular hole. C.E. Massonnet [11,12] carried out a limit analysis of a steel and concrete structure and, in another paper, presented complete solutions describing the limit state of reinforced concrete slabs. C.E. Massonnet and M.A. Save [13] published their book on the plastic analysis of structures. A nonlinear analysis of cylindrical shells with cutout was carried out by A. Brogan and B.O. Almroth [14]. M. Robinson carried out a comparison of various yield surfaces for thin shells [15] and a lower bound estimation of the limit pressure of a flush oblique cylindrical branch in a spherical pressure vessel was reported by M. Robinson and S.S. Gill [16]. An approximate solution to the lower bound limit load of cylindrical shells with a single cutout was found by S.S.B. Foo [17] and a good collection of works on the calculation of lower and upper bound limit loads of plates and shells are found in [18].

With the advancement of technology, the aerospace industry focused on strength to weight ratio as one of the main criteria and, in parallel, new requirements in the design of pressure vessels led to valuable studies on limit loads using computer aided calculations and finite element predictions, based on the elastic-plastic response of materials. In order to avoid complexity in the calculation of stresses and strains in a plastic state, lower and upper bound load calculations were studied by choosing statically admissible stress and kinematically admissible strain fields, respectively. Alternative approaches to the calculation of lower and upper bounds using a reduced modulus method were introduced, which, later on,

*. *Corresponding Author, Department of Mechanical Engineering, Tarbiat Modarres University, Tehran, I.R. Iran.*

1. *Department of Mechanical Engineering, Tarbiat Modarres University, Tehran, I.R. Iran.*

was modified by D.L. Marriot [19]. The method was further improved by D. Mackenzie and J.T. Boyle [20], via a method of estimating limit loads by iterative elastic analysis, called an elastic compensation method, using the conventional elastic finite element method. The method was initially derived for the calculation of lower bound limit loads and was then developed for the estimation of upper bound limit loads by D. Mackenzie et al. [21]. S.J. Hardy, A.R. Gowhari-Anaraki and M.K. Pipelzadeh found an estimation for upper and lower bound limits and shakedown loads for hollow tubes with axisymmetric internal projections under axial loading, using the elastic compensation method [22].

In this paper, square plates, with a single central hole under in-plane loading condition of various geometric and loading parameters, are studied. The limit load for each case is found by elastic-plastic finite element calculation, analytical limit load analysis and elastic compensation lower and upper bound methods, and their values are compared with results available in the literature. The main objective of this paper is to present analytical methods for the calculation of lower and upper bound limit loads for the cases studied and verify the suitability of elastic compensation lower and upper bound methods and the degree of accuracy of their results.

THEORETICAL CONSIDERATIONS

Yield Criteria In-Plane Stress State

The state of stress in any material element may be represented by a point in a nine-dimensional stress space. The external boundary of the elastic domain defines a surface known as the initial yield surface. Assuming that the material is initially isotropic, the plastic yielding depends only on the magnitudes of three principal stresses and not on their directions. For a given uniaxial yield stress, Y, the Tresca yield surface is a regular hexagon cylinder inscribed within the Von Mises cylinder. It is very well known that in case of in-plane loading, the plane stress state, where $\sigma_z = \sigma_{zy} = \sigma_{zx} = 0$, the Tresca yield surface is a hexagon inscribed within the Von Mises ellipse.

Von Mises yield criterion:

$$\sigma_1^2 - \sigma_1\sigma_2 + \sigma_2^2 = Y^2, \tag{1}$$

Tresca yield criterion:

$$\max.(|\sigma_1|, |\sigma_2|, |\sigma_1 - \sigma_2|) = Y. \tag{2}$$

Limit Theorems

In an elastic-plastic body subjected to a set of external forces, yielding begins in the most critically stressed element. By increasing the load, the plastic zone spreads, while deformation is restricted, due to constraint of the non-plastic material, until the constraint become locally ineffective and large plastic strains occur. If the material is non hardening and geometry change is ignored, the load approaches an asymptotic value, known as the limit load.

Lower Bound Theorem

If, for a given load (P_L), a statically admissible stress field exists satisfying stress boundary conditions and nowhere exceeding the yield stress of the material, then, (P_L) is a lower bound limit load.

Upper Bound Theorem

Assume a kinematically admissible velocity field satisfying the incompressibility condition, velocity boundary conditions and corresponding strain rates. The upper bound theorem states that the rate of work done by actual surface traction on the boundary is less than, or equal to, the rate of dissipation of internal energy in any kinematically admissible velocity field.

Finite Element Calculations

In this paper, two methods of limit analysis, based on finite element calculations using the ANSYS suite of programs, are employed, namely, the elastic-plastic method and the elastic compensation method, adopting the same finite element models for both methods.

Elastic-Plastic Method

In elastic-plastic calculation, the material is assumed to be isotropic and non hardening, obeying Von Mises yield criterion and the associated Prandtl-Ruess flow rules. In this method, the external load is applied to the model with default, maximum and minimum number of sub steps chosen as 50, 100 and 20, respectively. The model is subjected to an external load in an incremental manner each time until, due to an extensive spread of plastic state in the model and an unrestrained plastic flow, the model can no further resist even the slightest addition in external load, which is assumed to be the limit load of the model.

Elastic Compensation Method

In this method, an initial elastic finite element analysis is carried out with the plate under arbitrary external load (P_A). The iterative procedure starts from an initial elastic state of loading and redistributes the stresses in the model, decreasing maximum stress within the model until it can no further be reduced. The elastic modulus of each element is modified in each iteration, according to the ratio of limiting stress to element characteristic stress:

$$E^e_{(i+1)} = E^e_i \sigma_n / \sigma^e_i, \tag{3}$$

where $E^e_{(i+1)}$ and E^e_i are the new and current values of the elastic modulus, σ_n is the nominal stress value (here chosen to be 0.4 times the yield stress) and σ^e_i is the maximum nodal equivalent stress within the element (un-averaged) calculated in the current iteration. After each iteration, the stress is redistributed in the elements reducing maximum stress in the whole model until, theoretically, the maximum nodal equivalent stress within the model can be reduced no further or a converged value of maximum stress (σ_C) is reached. The convergence criterion is chosen as the ratio of $(\sigma^m_i - \sigma^m_{(i+1)})/\sigma^m_i$ to be equal to, or less than, some limiting value, where $\sigma^m_{(i+1)}$ and σ^m_i are the new and current maximum nodal equivalent stresses within the model, respectively. The main object of the redistribution of the stress within the element is to maximize the load carrying capacity of the plate with an applied external load, as far as it does not violate the Von Mises yield criterion. By applying the lower bound theorem, the lower bound limit load, (P_L), may be calculated as [22]:

$$P_L = P_A Y/\sigma_C. \tag{4}$$

and an upper bound estimation may be found by equating the dissipation energy (D_A) and the strain energy (U_A), corresponding to applied external load (P_A) [22]:

$$P_U = P_A D_A/U_A. \tag{5}$$

The value of strain energy may be found directly from the ANSYS output, while the dissipation energy is calculated from values of three principle strains, the yield stress and element volume, using the Von Mises yield criterion, based on absolute values of strains and not their rates:

$$D_A = Y\sqrt{[2(\varepsilon_1^2 + \varepsilon_2^2 + \varepsilon_3^2)/3]}, \tag{6}$$

where ε_i are the principal strains corresponding to applied external load (P_A).

Stress Concentration

Evaluation of the stress concentration factor for an infinite plate with an elliptic hole under an in-plane uniaxial load acting parallel to a minor axis was given by S.P. Timoshenko [23], using symbols introduced in this paper to be equal to $(1 + 2\rho/\mu)$, occurring at the end of a major axis of the hole and, in the case of a circular hole, where $\rho = \mu$, the stress concentration factor is found to be equal to three. It can also be shown that the stress concentration factor for an infinite plate with a circular hole under equal biaxial loading is equal to two [23]. The stress concentration factor at the edge of a small circular hole in a very large plate subjected to pure bending moment was given by R.E. Peterson [24] to be equal to $(5+3\nu)/(3+\nu)$, where ν is the Poisson's ratio.

LIMIT LOAD ANALYSIS OF PLATE WITH ELLIPTICAL HOLE UNDER UNIAXIAL TENSION

As the first example, a square plate with a central elliptical hole under uniaxial tension is considered. The ratio of major and minor diameters of the hole to plate width are ρ and μ, respectively, and the load is applied to vertical edges in a direction normal to the major diameter of the hole (Figure 1). In this section, at first, analytic estimations of the lower and upper bound limit load for both Von Mises and Tresca yield criteria are carried out, then, the results obtained, based on Von Mises criterion, are compared with elastic-plastic and elastic compensation method lower bound and upper bound values, using the finite element method.

Analytical Lower Bound Estimation

In order to obtain a lower bound solution for a plate with an elliptical hole, the quarter plate is divided into five regions of a constant stress state, with Region 5 assumed to be stress free, as shown in Figure 1. The geometrical parameter, ξ, indicates the position of the intersection of stress discontinuity lines of Regions 1-2 and 2-3. Assuming constant stress state, each region is in equilibrium, hence, it is only required to satisfy the stress boundary conditions, the jump conditions across stress discontinuity lines and corresponding yield criterion. Considering a statically admissible field and using the equality of normal and shear stresses on both sides of five stress discontinuity lines, as shown in Figure 1 and carrying out mathematical calculations, values of unknown principle stresses and angle α are

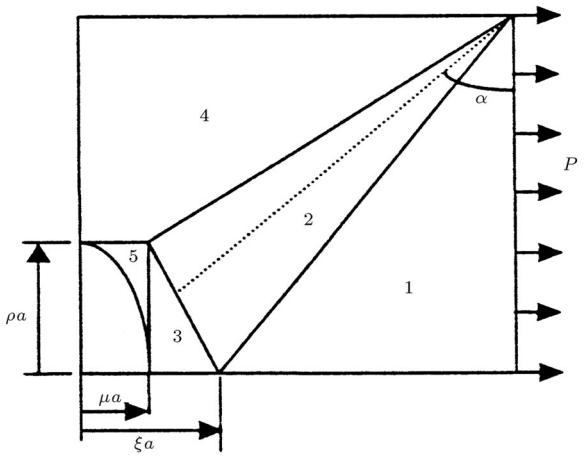

Figure 1. Quarter plate with elliptical hole under uniaxial tension, lower bound.

obtained as follows:

$$t_1 = P, \quad n_3 = t_4 = 0,$$

$$\tan(2\alpha) = 2\rho(1-\mu)/(-\rho^2+\mu^2-\mu+\xi+\rho-\mu\xi),$$

$$n_1 = \rho P/[(1-\xi)(1-\mu)],$$

$$n_2 - t_2 = CP/[(1-\mu)(\xi-\mu+\rho-\xi\rho)],$$

$$C = \sqrt{\{4\rho^2(1-\mu)^2 + [(\xi-\mu)(1-\mu)+\rho(1-\rho)]^2\}},$$

$$n_2+t_2 = [(1-\mu)(\xi-\mu)-\rho(1-\rho)]P/[(1-\mu)(\xi-\mu+\rho-\xi\rho)],$$

$$t_3 = -\rho P/[(1-\mu)(\xi-\mu)],$$

$$n_4 = P/(1-\rho), \tag{7}$$

where α is the angle between principal stress t_2 of Region 2 shown in Figure 1, acting in the direction of the dotted line and the vertical edge of the plate. The relations found in Equations 7 are functions of ρ, μ, ξ and P. By substituting obtained values of principal stresses in the Von Mises or Tresca yield criterion (Equations 1 and 2, respectively), lower bound limit loads for each region as functions of ξ are found.

Von Mises yield criterion:

$$\text{Region 1:} \quad P^* \leqq (1-\mu)(1-\xi)/\sqrt{\{\rho^2-\rho(1-\xi)(1-\mu)+(1-\xi)^2(1-\mu)^2\}},$$

$$\text{Region 2:} \quad P^* \leqq (1-\mu)(\xi+\rho-\mu-\xi\rho)/\sqrt{\{(1-\mu)^2((\xi-\mu)^2+3\rho^2)+\rho^2(1-\rho)^2+(\xi-\mu)(1-\mu)\rho(1-\rho)\}},$$

$$\text{Region 3:} \quad P^* \leqq (1-\mu)(\xi-\mu)/\rho,$$

$$\text{Region 4:} \quad P^* \leqq (1-\rho). \tag{8}$$

Tresca yield criterion:

$$\text{Region 1:} \quad P^* \leqq (1-\mu)(1-\xi)/\rho,$$

$$\text{Region 2:} \quad P^* \leqq (1-\mu)(\xi+\rho-\mu-\xi\rho)/\sqrt{\{4\rho^2(1-\mu)^2+[(\xi-\mu)(1-\mu)+\rho(1-\rho)]^2\}},$$

$$\text{Region 3:} \quad P^* \leqq (1-\mu)(\xi-\mu)/\rho,$$

$$\text{Region 4:} \quad P^* \leqq (1-\rho). \tag{9}$$

The parameter ξ is a variable with which the lower bound solution could be maximized. In order to find the best lower bound, each set of four equations is plotted for different values of ρ as functions of ξ (with known value of minor to major diameters ratio, μ, being fixed) and the greatest admissible value of P^* is found, which is the greatest ordinate of the region lying below all other curves.

The lower bound estimations for ρ, varying from 0 to 0.9 (at each 0.1 interval) with various (μ/ρ) ratios, are shown in Figures 2 and 3 for Von Mises and Tresca yield criteria, respectively. By setting $\mu = \rho$ (circular hole) the results match with the lower bound limit load for a plate with a circular hole found by P.G. Hodge [7]. It can be seen from Figures 2 and 3 that for each value of ρ and μ, the lower bound limit load, in the case

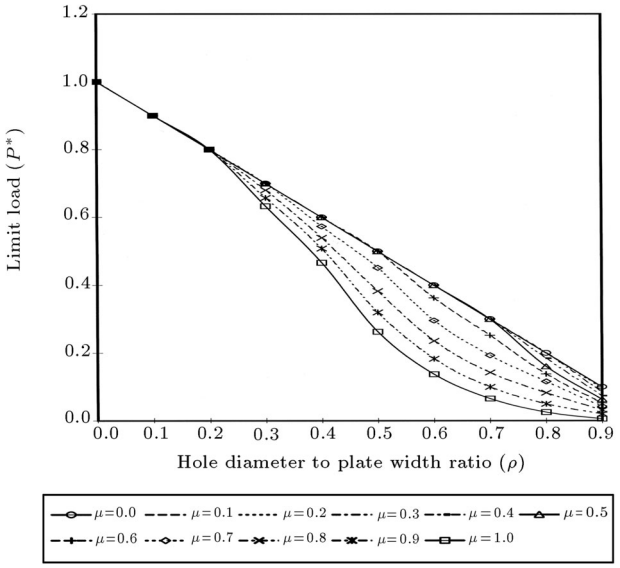

Figure 2. Square plate with elliptical hole at uniaxial tension, Von Mises criterion, lower bound.

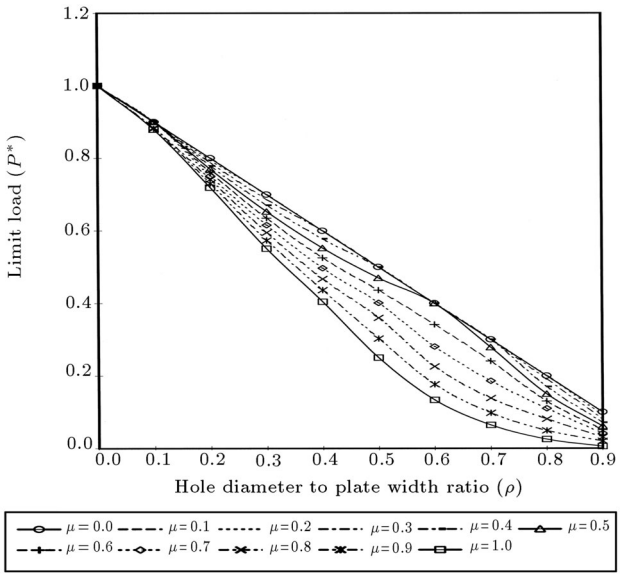

Figure 3. Square plate with elliptical hole at uniaxial tension, Tresca criterion, lower bound.

of the Tresca criterion, is either equal to or less and never more than that of the Von Mises criterion. It is also observed that as ρ increases, the lower bound limit load, P^*, decreases rapidly.

Analytical Upper Bound Estimation

In order to obtain an upper bound estimation for a plate with an elliptical hole, two modes of deformation (kinematically admissible fields) are considered, mode 1 as translational and mode 2 as rotational modes of deformation 18.

First Mode of Deformation

In the first mode of deformation (Figure 4), the upper and lower triangles are assumed to be rigid and move vertically inward. Let V be the velocity of one side of the neck relative to the other side and Ψ be the angle of inclination of neck to relative velocity. The rates of internal and external works per plate thickness are calculated and set equal, as per the Von Mises or Tresca yield criterion, in order to find an expression for the upper bound limit load. By differentiating the expression found with respect to β and Ψ, the solution is minimized:

Von Mises criterion:

$$\text{at } \beta = \pi/4 + \Psi/2 \quad \text{and} \quad \Psi = \sin^{-1}(1/3):$$

$$P^* = (1-\rho). \tag{10}$$

Tresca criterion:

$$\text{at } \beta = \pi/4 + \Psi/2 \text{ and } \Psi \text{ any value from 0 to } \pi/2:$$

$$P^* = (1-\rho). \tag{11}$$

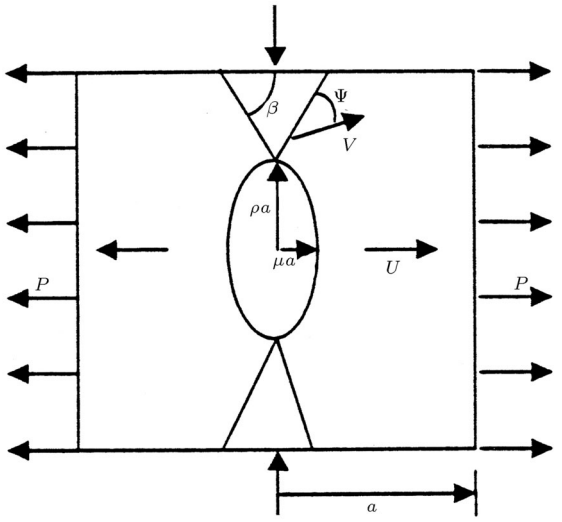

Figure 4. Square plate with elliptical hole under uniaxial tension, upper bound, first mode of deformation.

Second Mode of Deformation

In the second mode of deformation (Figure 5), each quarter plate is assumed to rotate with angular velocity, ω, about a point at distance ηa and ξa from x and y axes of the plate, respectively. The quarter plate shown is assumed to be rigid with necking and bulging at interface lines. The rates of internal and external work per plate thickness are calculated, as per Von Mises and Tresca yield criteria, and set equal to find an expression for the upper bound limit load. By differentiating the expression found with respect to ξ and η, the solution is minimized:

$$\text{at } 2\xi = 1+\mu \quad \text{and} \quad 2\eta = 1+\rho+\sigma/2K:$$

$$P/2K = -\rho + \sqrt{[\rho^2 + (1-\mu)^2 + (1-\rho)^2]}. \tag{12}$$

For a Von Mises material $K = Y/\sqrt{3}$ and for a Tresca material $K = Y/2$.

Hence, two upper bound limit loads found for the two modes of deformation are as follows:

Von Mises material:

$$P^* = (1-\rho),$$

$$P^* = 2\{-\rho + \sqrt{[\rho^2 + (1-\mu)^2 + (1-\rho)^2]}\}/\sqrt{3}, \tag{13}$$

Tresca material:

$$P^* = (1-\rho),$$

$$P^* = -\rho + \sqrt{[\rho^2 + (1-\mu)^2 + (1-\rho)^2]}. \tag{14}$$

The lowest values of two expressions in Equations 13 and 14 are the best upper bound estimations for

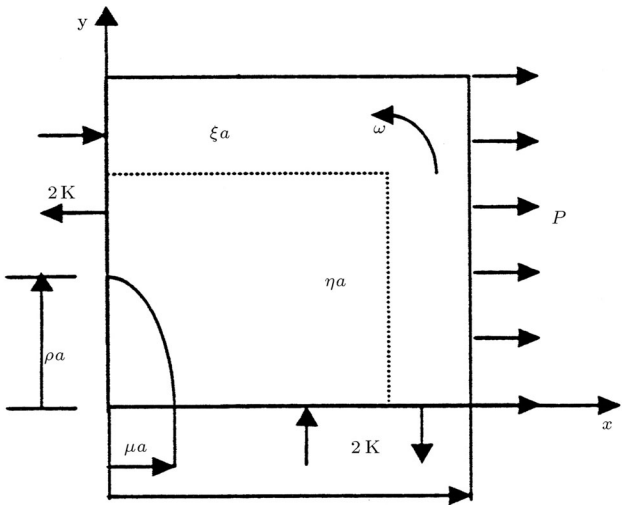

Figure 5. Square (quarter) plate with elliptical hole under uniaxial tension, upper bound, second mode of deformation.

different values of ρ (depending on value μ/ρ). It is noted that for small ratios of μ/ρ, the upper bound limit load corresponding to the first mode of deformation is less for all ranges of ρ ($\mu/\rho \leqq 0.59$ and $\mu/\rho \leqq 0.5$ for Von Mises and Tresca criteria, respectively). As the μ/ρ ratio increases, the upper bound limit load corresponding to the second mode of deformation becomes less for some mid ranges of ρ. Tables 1 and 2 show different ranges of ρ at which upper bound values corresponding to either of the two modes are less for Von Mises and Tresca criteria, respectively.

Upper bound estimations for ρ varying from 0 to 0.9 (at each 0.1 interval) with various (μ/ρ) ratios are shown in Figures 6 and 7 for Von Mises and Tresca yield criteria respectively. By setting $\mu = \rho$, the results match with the value of the upper bound limit load for a plate with a circular hole, as reported in [7,18]. In case of a lower bound limit load, it can be seen from

Table 1. Square plate with elliptical hole, uniaxial tension, better upper bound estimation (Von Mises criterion).

μ/ρ	First Mode	Second Mode
0.1	$0 \leqq \rho \leqq 1$	
0.2	$0 \leqq \rho \leqq 1$	
0.3	$0 \leqq \rho \leqq 1$	
0.4	$0 \leqq \rho \leqq 1$	
0.5	$0 \leqq \rho \leqq 1$	
0.6	$0 \leqq \rho \leqq 0.6876, 0.76 \leqq \rho \leqq 1$	$0.6876 \leqq \rho \leqq 0.76$
0.7	$0 \leqq \rho \leqq 0.5567, 0.916 \leqq \rho \leqq 1$	$0.5567 \leqq \rho \leqq 0.916$
0.8	$0 \leqq \rho \leqq 0.4927, 0.9662 \leqq \rho \leqq 1$	$0.4927 \leqq \rho \leqq 0.9662$
0.9	$0 \leqq \rho \leqq 0.4545, 0.9925 \leqq \rho \leqq 1$	$0.4545 \leqq \rho \leqq 0.9925$
1.0	$0 \leqq \rho \leqq 0.4216$	$0.4216 \leqq \rho \leqq 1$

Table 2. Square plate with elliptical hole, uniaxial tension, better upper bound estimation (Tresca criterion).

μ/ρ	First Mode	Second Mode
0.1	$0 \leqq \rho \leqq 1$	
0.2	$0 \leqq \rho \leqq 1$	
0.3	$0 \leqq \rho \leqq 1$	
0.4	$0 \leqq \rho \leqq 1$	
0.5	$0 \leqq \rho \leqq 1$	
0.6	$0 \leqq \rho \leqq 0.4905, 0.8616 \leqq \rho \leqq 1$	$0.4905 \leqq \rho \leqq 0.8616$
0.7	$0 \leqq \rho \leqq 0.4325, 0.9331 \leqq \rho \leqq 1$	$0.4325 \leqq \rho \leqq 0.9331$
0.8	$0 \leqq \rho \leqq 0.3896, 0.9275 \leqq \rho \leqq 1$	$0.3896 \leqq \rho \leqq 0.9275$
0.9	$0 \leqq \rho \leqq 0.3605, 0.9937 \leqq \rho \leqq 1$	$0.3605 \leqq \rho \leqq 0.9937$
1.0	$0 \leqq \rho \leqq 0.3333$	$0.3333 \leqq \rho \leqq 1$

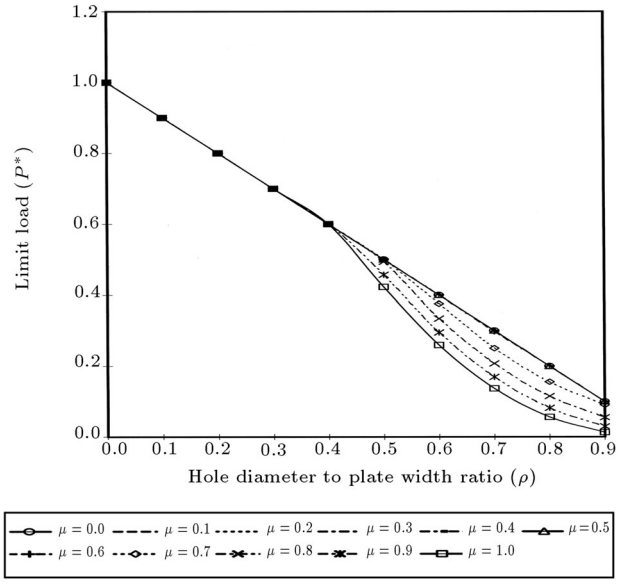

Figure 6. Square plate with elliptical hole at uniaxial tension, Von Mises criterion, upper bound.

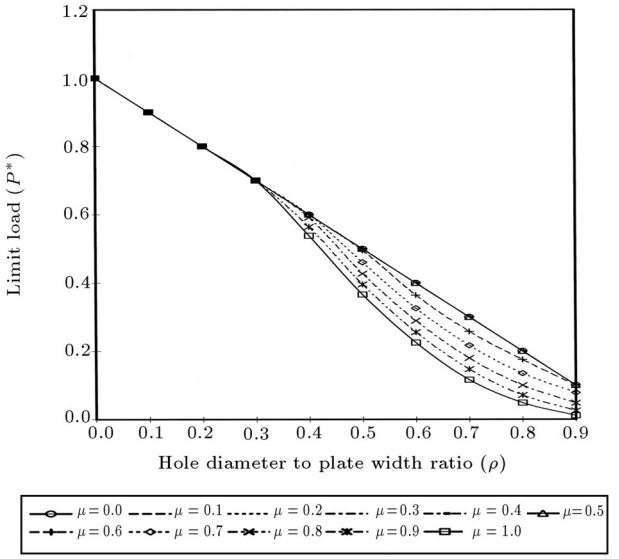

Figure 7. Square plate with elliptical hole at uniaxial tension, Tresca criterion, upper bound.

Figures 6 and 7 that for each value of ρ and μ the upper bound limit load, in case of the Tresca criterion, is either equal to or less and never more than that of the Von Mises criterion. Comparing lower and upper bound limit load estimations for both Tresca and Von Mises yield criteria (Figures 2, 3, 6 and 7), it is found that for smaller values of ρ, lower bound and upper bound results are the same, equal to $(1 - \rho)$, giving an exact limit load depending on the ratio of (μ/ρ) and, as ρ increase, their value departs from the line $(1 - \rho)$. This difference is more in magnitude and occurs at smaller ρ with an increase in (μ/ρ) ratio being maximum, in case of a circular hole, where $\mu = \rho$, which is shown by the lowest curves in Figures 4 to 7.

Finite Element Analyses

Finite element calculations were carried out considering a quarter plate of 0.2 m side length and 0.008 m thickness, using the advantage of symmetry at x and y axes. The quarter plate is divided into 15-12-12 divisions with 360 elements of a 4-noded structural element PLANE42 in ANSYS of the plane stress with a thickness option, as shown in Figure 8. The values of the initial elastic modulus, Poisson's ratio and nominal yield stress of the material were taken as 200E9 N/m^2, 0.3 and 300E6 N/m^2, respectively. The material is assumed to be isotropic and non hardening. In the elastic plastic method, the external load is applied to the model with default, the maximum and minimum number of sub steps chosen as 50, 100 and 20, respectively. If the model could resist an externally applied load, its magnitude will be increased at the next calculation time, as a result of which, the plastic state of the elements will spread and move further towards the external boundary of the plate until unrestrained plastic flow occurs and the model can no longer resist the slightest addition in external load, which is assumed to be the limit load of the model. The effect of increasing the number of divisions on the limit load estimation by the elastic plastic method was surveyed for the square plate with a circular hole under uniaxial tension, obeying the Von Mises criterion, as shown in Figure 9. It was found that for higher values of ρ, the limit load estimation is more sensitive to the number of elements, initially, but, as the number of elements increases, this sensitivity decreases and limit load versus number of element curves becomes flat, approaching some converged value.

In the case of the elastic compensation method, an arbitrary external load is applied to the model ensuring that all elements are within the elastic state. After carrying out a few iterations (within the range of 10 to 30 iterations) with value of nominal stress chosen as 0.4 times the nominal yield stress, the stress is redistributed in the elements, reducing the maximum nodal equivalent stress within the model until it reaches a converged value (σ_C). The convergence criterion, as described previously, is chosen to be equal to or less than 0.001. The lower and upper bound limit loads are then calculated with the help of Equations 4 and 5, respectively. It is interesting to note that in the case of the elastic compensation method, the adoption of finer meshing, e.g., 30-24-24 divisions with 1440 elements number, did not have a considerable effect on improving the result and even with the meshing of 6-6-5 divisions with 60 elements only, lower and upper bound estimations with a relatively similar degree of accuracy were obtained.

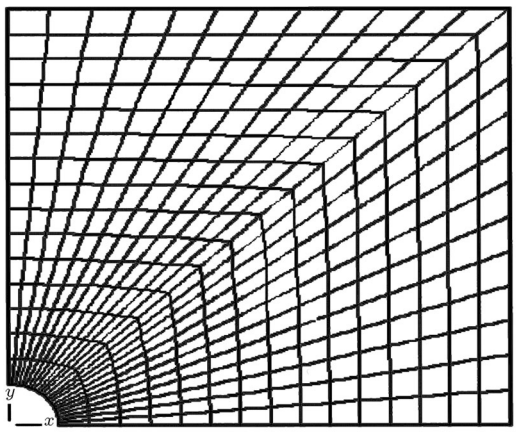

Figure 8. Quarter plate with circular hole 12-12-15 divisions, 360 4-noded structural PLANE42 elements.

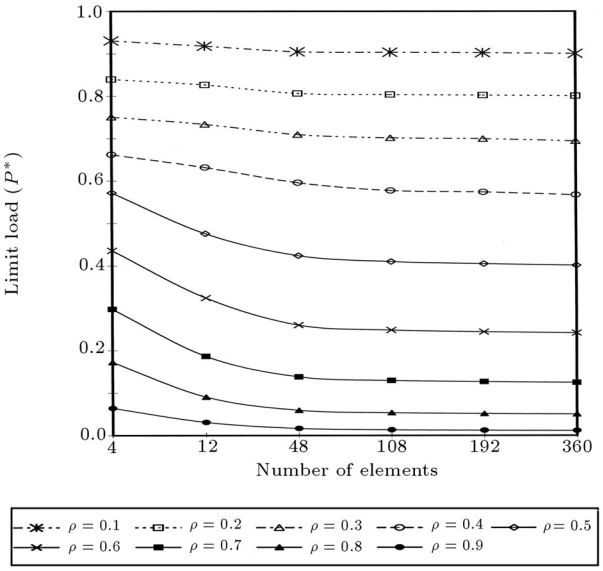

Figure 9. Variation of limit load with no. of elements, square plate with circular hole under uniaxial tension.

Three cases of plates with an elliptical hole under uniaxial tension with μ/ρ equal to 1, 0.5 and 0.05 are considered. Analytical and elastic compensation lower and upper bound values with elastic-plastic limit loads are calculated for ρ varying from 0 to 0.9 (at each 0.1 interval), which are shown in Figures 10 to 12, respectively. In the first case ($\mu/\rho = 1$), i.e., the plate with a circular hole (Figure 10), it is observed that for smaller values of ρ, where analytical lower and upper bounds are the same, giving the exact limit load, they are in good agreement with the elastic plastic results, but, as ρ increases, the analytical lower bound becomes more conservative and the analytical upper bound and elastic-plastic solutions are in better agreement. Lower bound limit loads found by the elastic compensation method are smaller than the analytical lower bound estimation for smaller values of ρ, but becoming more than the lower bound and getting closer to the upper bound value as ρ approaches 1.

In the second case ($\mu/\rho = 0.5$), the analytic upper

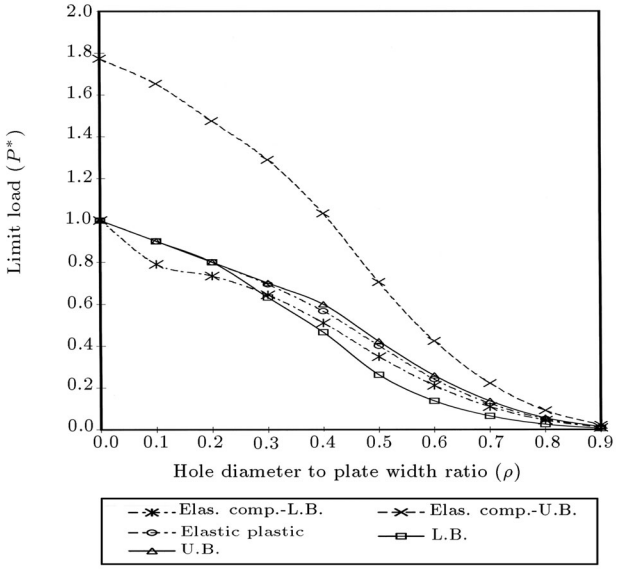

Figure 10. Square plate with circular hole under uniaxial tension, $\mu/\rho = 1$, Von Mises criterion.

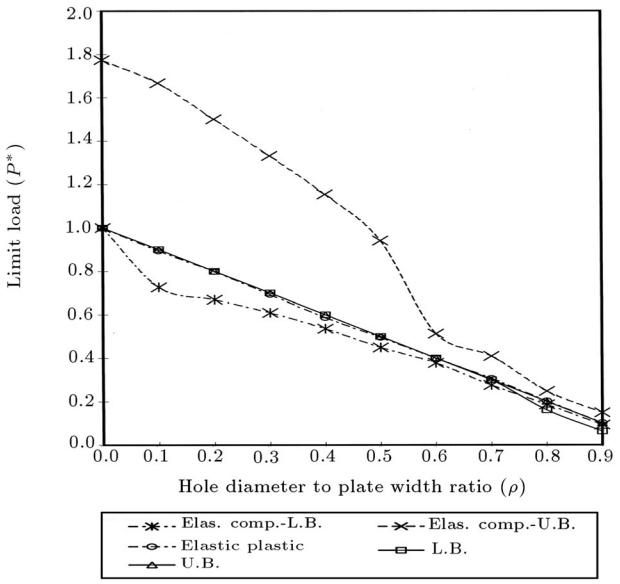

Figure 11. Square plate with elliptical hole under uniaxial tension, $\mu/\rho = 0.5$, Von Mises criterion.

and lower bound estimations are equal for a wide range of $\rho(\rho < 0.8)$, giving an exact value of the limit load and are in very good agreement with elastic-plastic results, while elastic compensation lower bound values differ from them at smaller values of ρ but improve as ρ approaches 1.

In the third case ($\mu/\rho = 0.05$), the analytical upper and lower bound estimations are equal for a whole range of ρ, obtaining an exact value of the limit load matching with the limit load found for a slab with a slit under uniaxial loading by P.G. Hodge [7]. These results also match with the limit load estimation of a plate with mid span crack under uniaxial tension in-

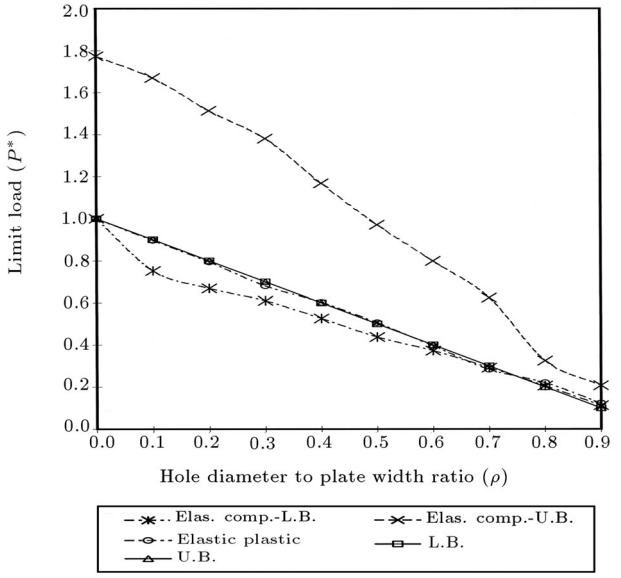

Figure 12. Square plate with elliptical hole under uniaxial tension, $\mu/\rho = 0.05$, Von Mises criterion.

plane stress condition given by T.L. Anderson [25]. The elastic-plastic results are in very good agreement with analytical upper and lower bound estimations except for $\rho > 0.8$, in which case elastic plastic results are slightly higher. The elastic compensation lower bound estimation has the same trend as in the second case.

In all three cases, the elastic compensation upper bound values are overestimated. The main reason for such overestimation may be due to the involvement of all elements within the whole model, rather than those elements which are a kinematically active portion of the structure participating in the plastic action.

LIMIT LOAD ANALYSIS OF PLATE WITH CIRCULAR HOLE UNDER BIAXIAL LOAD

As the second example, a square plate with a central circular hole under biaxial loading is considered. At first, an analytical estimation of the limit load is carried out, then, the results are compared with elastic-plastic and elastic compensation method lower bound and upper bound values.

Analytical Lower Bound Estimation

In this section, a square plate with a central circular hole under the action of biaxial load is considered, transverse load being a multiple of the axial load by λ, which ranges from -1 to 1 (Figure 13). In order to find the lower bound limit load, the quarter plate is divided into 7 regions of constant stress state, with Region 7 assumed to be stress free, as shown in Figure 13. Geometrical parameters, ξ and η, indicate the positions of intersection of stress discontinuity lines of Regions 1-2, 2-5 and 3-4, 4-6, respectively. Using the same

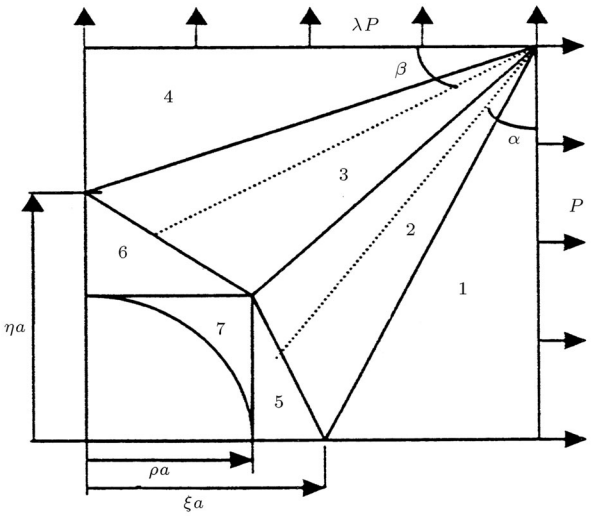

Figure 13. Quarter plate with circular hole under biaxial load, lower bound estimation.

analogy as previously described, unknown principle stresses and angles, α and β, are found as follows:

$$t_1 = P, \quad t_4 = \lambda P, \quad t_5 = t_6 = 0,$$

$$\tan(2\alpha) = 2\rho/[\xi(1-\lambda)],$$

$$\tan(2\beta) = 2\rho\lambda/[\eta(1-\lambda)],$$

$$n_1 = [\rho + \lambda(1-\xi)]P/[(1-\rho)(1-\xi)],$$

$$n_2 - t_2 = \sqrt{[4\rho^2 + \xi^2(1-\lambda)^2]P/[\xi(1-\rho)]},$$

$$n_2 + t_2 = [2(\xi-\rho) - \xi(1-\lambda)]P/[\xi(1-\rho)],$$

$$n_3 - t_3 = \sqrt{[4\rho^2\lambda^2 + \eta^2(1-\lambda)^2]P/[\eta(1-\rho)]},$$

$$n_3 + t_3 = [\eta(1+\lambda) - 2\rho\lambda]P/[\eta(1-\rho)],$$

$$n_4 = (1 - \eta + \rho\lambda)P/[(1-\eta)(1-\rho)],$$

$$n_5 = -[\rho + \lambda(\rho-\xi)]P/[(1-\rho)(\xi-\rho)],$$

$$n_6 = -(\rho\lambda + \rho - \eta)P/[(1-\rho)(\eta-\rho)], \qquad (15)$$

where α is the angle between principal stress t_2 of Region 2 shown acting in the direction of the dotted line at the vertical edge of the plate and β is the angle between principal stress t_3 of Region 3 shown acting in the direction of the dotted line at the horizontal edge of the plate. By substitution of obtained values of principal stresses in Von Mises and Tresca yield criteria (Equations 1 and 2, respectively), concerned lower bound limit loads for each region are found as functions of ρ, λ, ξ and η. It should, however, be noted that in case of negative λ, the buckling criterion was not considered in this analysis.

Von Mises yield criterion:

Region 1: $P^* \leqq (1-\rho)(1-\xi)/$

$$\sqrt{\{\rho^2 - \rho(1-\xi)(1-\rho) + (1-\xi)^2(1-\rho)^2 + \lambda(1-\xi)[2\rho - (1-\rho)(1-\xi)] + \lambda^2(1-\xi)^2\}},$$

Region 2: $P^* \leqq \xi(1-\rho)/$

$$\sqrt{\{4\rho^2 + \xi^2(1-\lambda)^2 - \rho\xi(1+\lambda) + \lambda\xi^2\}},$$

Region 3: $P^* \leqq \eta(1-\rho)/$

$$\sqrt{\{4\rho^2\lambda^2 + \eta^2(\lambda-1)^2 - \rho\lambda\eta(1+\lambda) + \lambda\eta^2\}},$$

Region 4: $P^* \leqq (1-\rho)(1-\eta)/$

$$\sqrt{\{(1-\eta)^2 + \lambda(1-\eta)[2\rho - (1-\rho)(1-\eta)] + \lambda^2[\rho^2 - \rho(1-\rho)(1-\eta) + (1-\eta)^2(1-\rho)^2]\}},$$

Region 5: $P^* \leqq (1-\rho)(\xi-\rho)/[(\lambda(\xi-\rho) - \rho)],$

Region 6: $P^* \leqq (1-\rho)(\eta-\rho)/[(\rho\lambda + \rho - \eta)]. \qquad (16)$

Tresca yield criterion:

Region 1: $P^* \leqq (1-\rho)(1-\xi)/[\rho + \lambda(1-\xi)],$

Region 2: $P^* \leqq \xi(1-\rho)/\sqrt{\{4\rho^2 + \xi^2(1-\lambda)^2\}},$

Region 3: $P^* \leqq \eta(1-\rho)/\sqrt{\{4\rho^2\lambda^2 + \eta^2(\lambda-1)^2\}},$

Region 4: $P^* \leqq (1-\rho)(1-\eta)/|(1-\eta+\rho\lambda)|,$

Region 5: $P^* \leqq (1-\rho)(\xi-\rho)/|(\rho + \lambda(\rho-\xi)|,$

Region 6: $P^* \leqq (1-\rho)(\eta-\rho)/|(\rho\lambda + \rho - \eta)\}|. \qquad (17)$

The best lower bound is found by plotting each set of six equations for specific values of λ and ρ as functions of ξ and η and finding the greatest admissible value of P^*, which is the greatest of the ordinates of the region lying below all other curves. By setting $\lambda = 0$, the above expressions match the results, in the case of a plate with a circular hole under uniaxial load [7].

Upper Bound Estimation

In order to obtain an upper bound solution, two modes of deformation (kinematically admissible fields) are considered; mode 1 as translational and mode 2 as rotational, as previously described.

First Mode of Deformation

Considering the first mode of deformation, by equating the rates of internal and external work per plate thickness and differentiating the expression for the upper bound limit load ratio, with respect to β and Ψ, the solution is minimized:

Von Mises criterion,

at $\beta = \pi/4 + \Psi/2$ and

$$\Psi = \sin^{-1}\{[1+\lambda(1-\rho)]/3[1-\lambda(1-\rho)]\}:$$

$$P^* = (1-\rho)/\sqrt{[1-\lambda(1-\rho)+\lambda^2(1-\rho)^2]}. \quad (18)$$

Tresca criterion,

at $\beta = \pi/2$ and $\Psi = \pi/2$:

$$P^* = (1-\rho). \quad (19)$$

Second Mode of Deformation

Considering the second mode of deformation, by equating the rates of internal and external work per plate thickness and differentiating the expression for the upper bound limit load ratio, with respect to ξ and η, the solution is minimized:

at $2\xi = 1+\rho-\lambda\sigma/2K$ and

$$2\eta = 1+\rho+\sigma/2K:$$

$$P/2K = \{-\rho(1-\lambda) + \sqrt{[\rho^2(1-\lambda)^2+2(1+\lambda^2)(1-\rho)^2]}\}/(1+\lambda^2). \quad (20)$$

For a Von Mises material: $K = Y/\sqrt{3}$ and for a Tresca material: $K = Y/2$.

Hence, two solutions obtained for upper bound limit loads are compared for different values of ρ and the best solution is found:

Von Mises material:

$$P^* = (1-\rho)/\sqrt{[1-\lambda(1-\rho)+\lambda^2(1-\rho)^2]},$$

$$P^* = 2/\sqrt{3}\{-\rho(1-\lambda) + \sqrt{[\rho^2(1-\lambda)^2+2(1+\lambda^2)(1-\rho)^2]}\}/(1+\lambda^2). \quad (21)$$

Tresca material:

$$P^* = (1-\rho),$$

$$P^* = \{-\rho(1-\lambda) + \sqrt{[\rho^2(1-\lambda)^2+2(1+\lambda^2)(1-\rho)^2]}\}/(1+\lambda^2). \quad (22)$$

By setting $\lambda = 0$, the above expressions match with the case of a plate with a circular hole under uniaxial load.

Square Plate with Circular Hole Under Equal Biaxial Load

When the plate is subjected to a uniform normal stress along all its edges, an exact solution is found for a Von Mises material for a range of $0.483 \leqq \rho \leqq 1$ [18]:

$$P^* = 2/\sqrt{3}\sin(\alpha - \pi/6),$$

$$\rho^2 = 2/\sqrt{3}\cos\alpha e^{-\sqrt{3(\alpha-\pi/6)}}. \quad (23)$$

For values of $0 \leqq \rho \leqq 0.483$, the above equation is lower bound, since the stress field is statically admissible. The upper bound limit loads are found as [18]:

$$0.1429 \leqq \rho \leqq 0.483, \quad P^* = 2/\sqrt{3}(1-1.035\rho), \quad (24)$$

$$0 \leqq \rho \leqq 0.1429, \quad P^* = (1-\pi\rho^2/4). \quad (25)$$

In case of material obeying the Tresca yield criterion, the upper and lower bounds are the same, giving an exact solution for all ranges of ρ/a as [18]:

$$P^* = (1-\rho). \quad (26)$$

In this section, four cases of plates with a circular hole under biaxial loading, with λ equal to $1, 0.5, -0.5$ and -1 are studied and the results are shown in Figures 14 to 17, respectively. Analytical and elastic compensation lower and upper bound values with elastic-plastic limit loads are calculated for ρ varying from 0 to 0.9 (at each 0.1 interval). Finite element calculations were carried out in a similar manner to

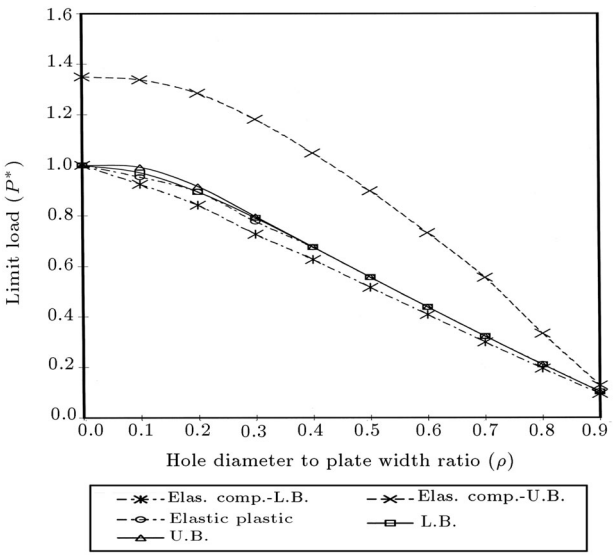

Figure 14. Square plate with circular hole under equal biaxial tension, $\lambda = 1$, Von Mises criterion.

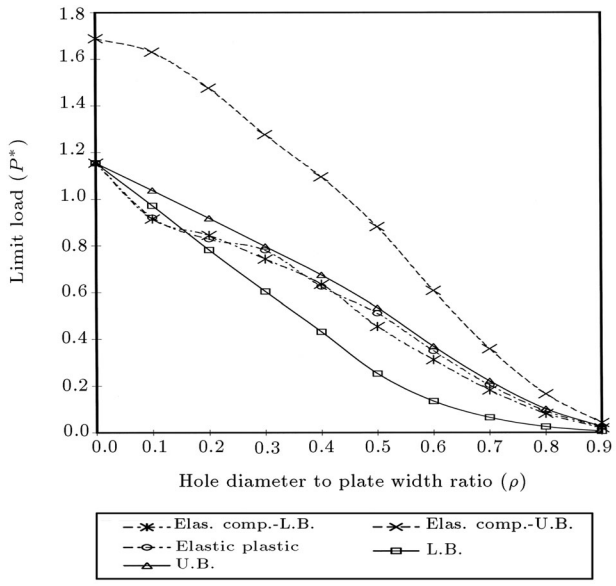

Figure 15. Square plate with circular hole under biaxial load, $\lambda = 0.5$, Von Mises criterion.

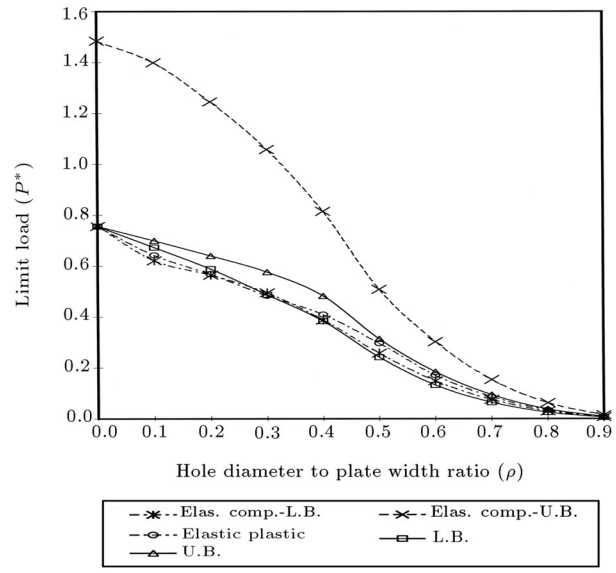

Figure 16. Square plate with circular hole under biaxial load, $\lambda = -0.5$, Von Mises criterion.

that described in the previous section. In the first case of equal biaxial loading ($\lambda = 1$), comparing the lower bound limit load estimated in the previous section with those obtained in this section with $\lambda = 1$, it is noted that the former results are under estimated. Hence, the results in this section are used to be compared with finite element calculations. In this case ($\lambda = 1$), the elastic-plastic solution is in very good agreement with exact results for a range of $0.483 \leqq \rho/a \leqq 1$ and, for smaller values of ρ, it is very close to the analytical lower bound estimation, while the elastic compensation lower bound values are slightly lower than elastic-plastic solutions.

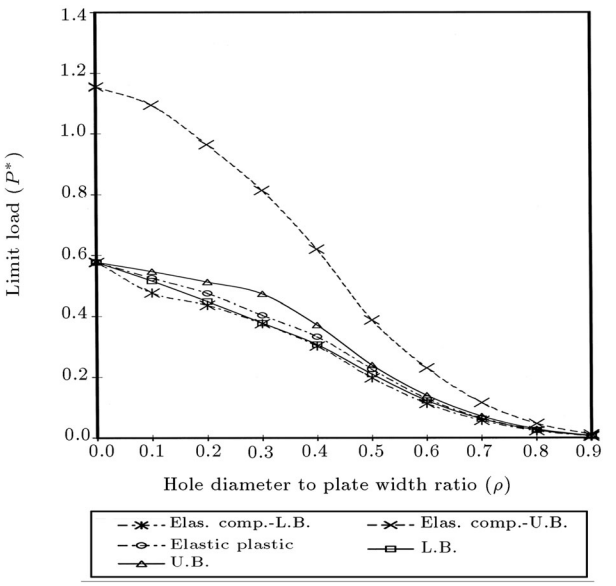

Figure 17. Square plate with circular hole under biaxial load, $\lambda = -1$, Von Mises criterion.

For the second case ($\lambda = 0.5$), the elastic-plastic results are closer to the analytical lower bound for smaller values of $\rho(\rho \leqq 0.2)$ and to the analytical upper bounds for larger values of $\rho(\rho > 0.2)$, while the elastic compensation lower bound values are in good agreement with elastic-plastic results. In the third case of biaxial loading ($\lambda = -0.5$), the elastic-plastic results are closer to the analytical lower bound estimation for $\rho \leqq 0.4$ (being lower in value for $\rho \leqq 0.3$) and to analytical upper bounds for $\rho > 0.4$. The elastic compensation lower bound values are found to be in good agreement with elastic-plastic results. In the fourth case of biaxial loading ($\lambda = -1$), the elastic-plastic results are closer to the analytical lower bound for $\rho \leqq 0.4$ and are nearly equal to the mean value of the analytical lower and upper bound limits for $\rho > 0.4$, with the elastic compensation lower bound estimations being in good agreement with elastic-plastic results. As could be expected, in all four cases of the biaxial loadings studied, the elastic compensation upper bound values are overestimated.

CONCLUSION

In this paper, lower and upper bound limit load estimations for a plate with a central hole of various sizes and under different in-plane loading conditions were carried out by analytical calculations, the elastic compensation method and, then, compared with elastic plastic results. The main conclusions are as follows:

1. In cases of plates with an elliptic hole under the action of uniaxial load, lower bound and upper bound limit loads are the same and equal to $(1-\rho)$, giving an exact limit load for smaller values of ρ, which depends on the (μ/ρ) ratio and, as ρ

increases, their value departs from the line $(1-\rho)$. This difference is more in magnitude and occurs at smaller ρ with an increase in (μ/ρ) ratio, being maximum in cases of circular holes, where $\mu = \rho$. The analytical upper and lower bound estimations and elastic-plastic results are in very good agreement with elastic compensation lower bound values differing at smaller values of ρ but getting closer as ρ approaches 1. The elastic compensation upper bound values are overestimated;

2. Considering various cases of plates with a circular hole under biaxial in-plane loads of ratio λ and with an elliptical hole under the uniaxial load studied, by comparing the estimated values of limit loads by different methods, it is noted that the lower bound limit loads found by the elastic compensation method are in good agreement with the analytical estimations of limit load and elastic-plastic results;
3. The upper bound values found by the elastic compensation method are, generally, of higher values than analytical or elastic plastic solutions. As stated, the main reason for such overestimation could be due to the involvement of all elements within the whole model rather than those elements which are a kinematically active portion of the structure participating in the plastic action. Hence, an improvement in the upper bound limit load estimation by the elastic compensation method is expected by adoption of a kinematically active portion of the structure rather than the whole model;
4. A fairly good result may be obtained by the elastic compensation lower bound method, even with relatively coarser finite element meshing and few iteration steps, compared with the case of elastic plastic computation, in which finer meshing and an increased number of sub steps are required to obtain reasonably accurate results;
5. In the case of the elastic compensation method, convergence is not always strictly positive, especially with an increasing hole diameter to plate width ratio, in which it was observed that either the upper bound limit load tends to zero or becomes lower than the lower bound value after some iteration or the rate of reduction of maximum stress becomes unstable.

NOMENCLATURE

ρ	ratio of hole major diameter to plate width
μ	ratio of hole minor diameter to plate width
P	applied load (stress) at the plate edge
λ	ratio of transverse load (stress) to axial load (stress)
Y	yield stress(normal)
K	yield stress(shear)
σ	stress
ε	strain
n_i, t_i	principal stresses of constant stress (Region i)
E	modulus of elasticity (Young's modulus)
P_A	arbitrary applied external load
P_L	lower bound limit load estimation
P_U	upper bound limit load estimation
σ_C	converged value of maximum stress in the model
σ_n	nominal stress value
σ^e	maximum nodal equivalent stress within the element
σ^m	maximum nodal equivalent stress within the model
D_A	dissipation energy due to applied load
U_A	strain energy due to applied load
P^*	non-dimensional limit load (P/Y)

REFERENCES

1. Kirsch, G. "Die theorie der elastizitat und die bedurfnisse der festigkeitslehre", *Veit. Ver. Deut. Ing*, **42**, pp 797-807 (1898).
2. Savin, G.N., *Stress Concentration Around Holes*, Pergamon Press, Oxford (1961).
3. Peterson, R.E., *Stress Concentration Design Factors*, John Wiley, New York, USA (1974).
4. Chong, K.P. and Pinter, W.J. "Stress concentration of tensile strips with large holes", *Computers and Structures*, **19**(4), pp 583-589 (1984).
5. Hodge, P.G. Jr. and Froyd, R.K. "The reinforcement to full strength of a thin slab with a slit", DAM Rept. B11-10, Brown University, Providence, USA (1953)
6. Hodge, P.G. Jr. "Final report on yield loads of slabs with reinforced cut outs", DAM Rept. B11-22, Brown University, Providence, USA (1953)
7. Hodge, P.G. Jr., *Plastic Analysis of Structures*, McGraw-Hill book company (1959).
8. Hodge, P.G. Jr., *Limit Analysis of Rotationally Symmetric Plates and Shells*, Prentice-Hull, Inc. (1963).
9. Gaydon, F.A. "On the yield-point loading of a square plate with concentric circular hole", *J. Mech. and Phys. Solids*, **2**, pp 170-176 (1954).
10. Gaydon, F.A. and McCrum, A.W. "A theoretical investigation of the yield point loading of a square plate with a central circular hole", *J. Mech. and Phys. Solids*, **2**(156) (1954).

11. Massonnet, C.E. "Limit design applied to steel and concrete structures", (lecture notes) University of California, Civil Eng. Dept. (1965).

12. Massonnet, C.E. "Complete solutions describing the limit state of reinforced concrete slabs", *Mag. Conc. Research*, **19**, 58, 13, (March 1967).

13. Massonnet, C.E. and Save, M.A. "Calcul. plastique des constructions (plastic analysis of structures)", **1 & 2**, Brassels (1963).

14. Brogan, A. and Almroth, B.O. "Buckling of cylinders with cutouts", *AIAA J.*, **8**(2), pp 236-241 (1970).

15. Robinson, M. "A comparison of yield surfaces for thin shells", *Int. J. Mech. Sci.*, **13** (1971).

16. Robinson, M. and Gill, S.S. "Lower bound to the limit pressure of flush oblique cylindrical branch in a spherical pressure vessel", *Int. J. Mech. Sci.* (1972).

17. Foo, S.S.B. "On the limit analysis of cylindrical shells with a single cutout", *Int. J. Press. Ves. & Piping*, **49**, pp 1-16 (1992).

18. Chakrabarty, J., *Applied Plasticity*, Springer (1999).

19. Marriot, L.D. "Evaluation of deformation or load control of stresses under inelastic conditions using elastic finite element stress analysis", In *Proceedings of the Pressure Vessels and Piping Conference*, Pittsburgh, Pennsylvania, **PVP-136**, American Society of Mechanical Engineers, New York, USA (1988).

20. Mackenzie, D. and Boyle, J.T. "A method of estimating limit loads by iterative elastic analysis. I: simple examples", *Int. J. Pressure Vessels Piping*, **53**, pp 77-95 (1993)

21. Mackenzie, D., Nadarajah, C., Shi, J. and Boyle, J.T. "Simple bounds on limit loads by elastic finite element analysis", *Trans. ASME, J. Pressure Vessels Technol.*, **115**, pp 27-31 (1993).

22. Hardy, S.J., Gowhari-Anaraki, A.R. and Pipelzadeh, M.K. "Upper and lower bound limit and shakedown loads for hollow tubes with axisymmetric internal projections under axial loading", *Journal of Strain Analysis*, **36**(6), pp 595-604 (2001).

23. Timoshenko, S.P. and Goodier, J.N., *Theory of Elasticity*, McGraw-Hill Book company (1951).

24. Peterson, R.E., *Stress Concentration Factors*, Wiley, New York, USA (1974).

25. Anderson, T.L., *Fracture Mechanics, Fundamentals and Applications*, CRC Press LLC (1995).